# Floating Wind Farm Layout Optimization Considering Moorings and Seabed Variations



Journal of Physics: Conference Series **2767** (2024) 062038 doi:10.1088/1742-6596/2767/6/062038

# Floating Wind Farm Layout Optimization Considering Moorings and Seabed Variations

**Matthew Hall[1], Michael Biglu[1], Stein Housner[1], Katherine Coughlan[1], Mohammad Youssef Mahfouz[2], Ericka Lozon[1]**

[1] National Renewable Energy Laboratory (NREL), 15013 Denver W Pkwy, Golden, CO 80401, United States

[2] Stuttgart Wind Energy at University of Stuttgart, Allmandring 5B, 70569 Stuttgart, Germany

E-mail: matthew.hall@nrel.gov

**Abstract.** This paper presents a method for optimizing the layout of floating wind farms that accounts for realistic seabed variations and the consequent adjustments to the mooring systems required for different turbine positions. The mooring lines of floating wind farms create large spatial constraints that are depth-dependent, since mooring designs must adapt to variations in seabed conditions over the array area. We develop a layout optimization methodology that addresses this, adjusting mooring system designs based on the local seabed characteristics as the layout changes and using steady-state models for the wake effects and mooring lines. The approach includes design algorithms that adjust the anchor positions and line length to achieve the desired mooring line profile for different water depths, and a layout optimization framework that implements spatial constraints between the turbines, mooring lines, and lease area boundaries. Demonstrating the method on several cases shows the effect of the seabed and spatial-constraint factors, as well as their interactions, on the optimal array layout. This demonstration paves the way for scaling up the method, using more powerful optimization algorithms to handle larger farm sizes and situations with more intensely varied seabed conditions.

## 1. Introduction

Designing the layout of floating offshore wind farms is more complicated than for other wind farms because of platform motions, the large footprint of the mooring systems, and the seabed dependence of mooring systems. While all wind farm optimization problems involve managing wake effects and spatial constraints (such as site boundaries or exclusion areas), floating wind farm optimization must also deal with platform offsets and design-dependent mooring positioning constraints. For example, a floating wind turbine's mooring system can be rotated to fit closer to an array boundary or avoid crossing mooring lines or power cables from another turbine.

In sites with significant depth variations, layout adjustments can change the depth of an anchor point and require changing the horizontal distance between the anchor and the turbine. These interactions make it important that layout optimizations for floating wind farms consider seabed variations and position-dependent adjustments of mooring line designs.

There are many papers on layout optimization of wind farms (e.g., [1, 2, 3, 4, 5, 6]), and a number of studies on layout optimization specific to offshore wind farms (e.g., [7, 8, 9]). Within this literature, methods for optimizing turbine positions within a bounded area are well

established. Criado Risco et al. demonstrate the use of inclusion and exclusion boundaries in a gradient-based optimization [3]. In an example of including seabed variability, Liu et al. [7] used a genetic-algorithm layout optimization for fixed-bottom wind turbines over varied seabed terrain (bathymetry) and found that including the seabed variability increased the cost of energy by around 25%.

Some recent studies have looked into optimizing floating wind farm layouts. Diaz et al. [6] developed an approach for placing turbines within a lease area based on a mix of technical and space-use constraints. Rapha [10] developed a layout optimization tool that includes some prescribed adjustment to mooring and cabling designs based on depth variations. Lerch et al. [10][11] developed a method for floating wind farm layout optimization focusing on array cable costs and losses. Mahfouz et al. [12] looked at layout optimization considering moorings and wake effects on uniform seabeds. Froese et al. [13] applied an iterative optimization to optimize the layout of a floating offshore wind farm, considering a specific water depth and wind rose. Several recent studies by Mahfouz et al. [12]), Liang and Liu [14] and Serrano Gonzales et al. [15] investigate use of mooring systems intentionally designed to cause lateral offsets that can reduce wake effects. While these studies address many aspects of floating wind farm layout optimization, the engineering requirements for adjusting mooring systems over a site's varied seabed conditions have been addressed very little. A recent example is from Hietanen et al. [16], who consider a floating wind farm optimization considering mooring lines and power cables over varied seabed conditions that include a binary handling of areas of bedrock.

In this paper, we aim to continue progress in integrating mooring design into layout optimization, with an approach that includes adjustment and evaluation of every mooring line and anchor based on spatially varying seabed conditions.

## 2. Methodology

A design optimization approach for floating wind farm layout and mooring systems needs to include models that predict performance, design algorithms that perform automatic design and optimization on subsystems, and an overall layout optimization algorithm that coordinates the search for optimal solutions. We created an approach that includes each of these elements in a somewhat simplified form, allowing for efficient exploration of this challenging optimization problem area. Each element is capable of handling a realistic site-specific scenario in terms of various mooring system configurations, seabed soil and depth variations, irregular boundary conditions, turbine thrust curves, and site wind resource data. However, we explore this approach using relatively simple models and site scenarios to produce simpler and clearer initial results.

Modeling of the array is provided by a combination of two models. MoorPy [17] is a quasi-static mooring model that supports any mooring line and dynamic cable configurations, multiple floating systems, and seabed bathymetry. It models the mooring systems and is used to compute their costs. FLORIS [18] is a wind farm flow tool for modelling and optimizing wind farms with various steady state wake models. We used the Guass-curl hybrid wake model [19] in this work to compute annual energy production (AEP) based on a provided wind rose (Figure 1a).

### *2.1. Layout Parameterization*

Optimizing the layout of a floating wind farm requires the typical design variables for wind farm layout—each turbine's x and y coordinate—as well as design variables that describe the mooring system layout. To avoid unusual mooring arrangements and to keep things simple, we assume that the mooring systems will each consist of three mooring lines with uniformly spaced headings. The anchor position and configuration details of each mooring line will be handled deterministically by a separate process (described in Section 2.2). Therefore, the only additional

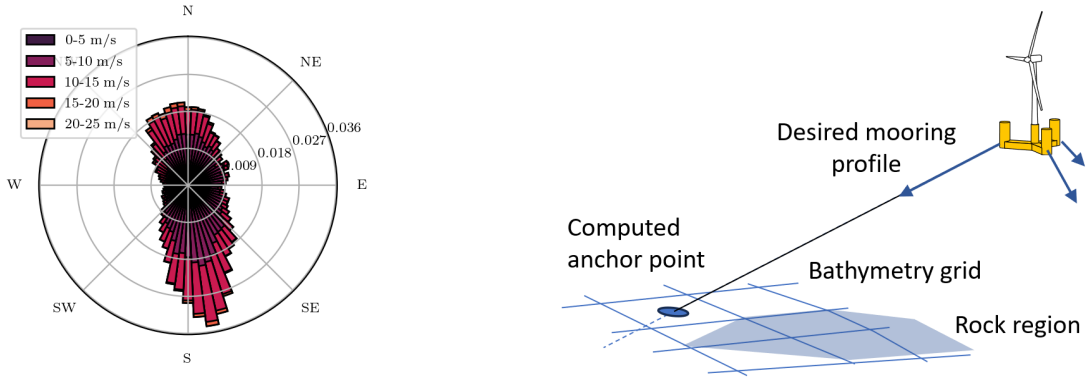


(a) Wind velocity distribution (b) Anchor positioning based on desired mooring line profile

Figure 1: Site-specific spatial factors considered in the layout optimization

design variable need for the mooring layout is a heading offset, which shifts the headings of a turbine's three mooring lines.

Each of the $n$ floating wind turbines in the array then has three layout design variables: x coordinate, y coordinate, and mooring heading ($\phi$). The heading zero corresponds to a mooring line facing along the positive x direction and rotations are counterclockwise (Figure 2).

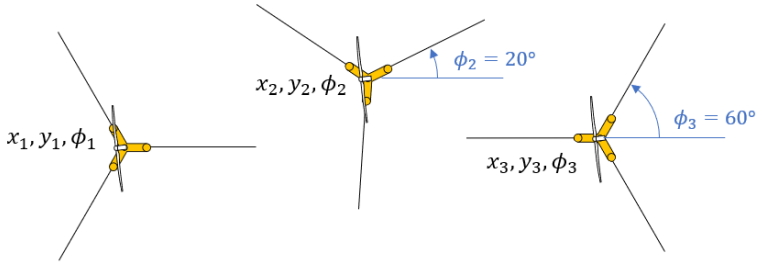


Figure 2: Layout parameters (design variables)

### *2.2. Mooring Design Algorithms*

Several interconnected design algorithms provide an automatic adjustment for components in the array as the layout changes and the seabed conditions under the components vary. The approach supposes that an initial viable mooring system has been provided, and that it should be adjusted to achieve similar performance measures when dealing with changes in seabed depth.

- Anchor positioning: To compensate for variations in the seabed depth, each anchor's position is selected using an algorithm that finds the point on the seabed that will give the desired mooring line profile (as specified by the user). The approach takes a desired mooring line profile shape (linear is used in the present study) and computes its intersection with the seabed bathymetry grid (Figure 1b).
- Mooring line sizing: For a given initial mooring configuration, as the water depth and anchor position varies, each mooring line is adjusted to meet the same horizontal pretension (the horizontal component of fairlead tension when the platform is undisplaced) as the original mooring design. This adjustment is done by adjusting the unstretched length of the rope of the mooring line, using a Newton's method solver with MoorPy in the loop until

the pretension converges. Matching the horizontal pretension is necessary for keeping the desired equilibrium turbine positions.

- Anchor sizing: For a given anchor type, the anchor size is adjusted to achieve the required holding capacity based on the soil properties at the anchor's location on the seabed grid.

In the current implementation, we take a simplification that is reasonable for taut mooring systems in deep water. We begin with a well-designed taut mooring system for the average water depth. Then, we assume that suitable designs for shallower or deeper water will have the same line declination angle, thus the only design adjustment required is to adjust the length to maintain the same pretension. This results in a small variation in system stiffness and dynamic tensions, roughly proportional to depth. In deep water, these variations are relatively mild.

Because it is a taut mooring design where there is no seabed contact, the design can be entirely a function of water depth. In contrast, a catenary or semi-taut design has some length on the seabed and would therefore depend on seabed slope, which would add more variables for the mooring design algorithm. In either case, desired mooring system properties (e.g., undisplaced pretension and declination angle) can be precomputed, and then algorithms can efficiently adjust the mooring design to maintain those properties in the layout optimization loop. More sophisticated approaches could optimize the mooring line headings or sizes based on the directional distribution of environmental conditions; however, we did not consider this degree of design variation in the present work.

### *2.3. Spatial Constraints*

The main spatial constraints when considering the floating wind turbines and mooring systems are related to ensuring that the turbines and moorings keep a safe distance from each other and from the lease area boundary. These considerations are contained in three constructs:

- Wind turbine buffer zone: an area around each wind turbine's undisplaced position that should be kept clear to avoid risk of collision with the wind turbine. We set this radius to be 480 m (twice the rotor diameter), as an approximation of clearance necessary for the rotor size as well as the potential offsets of the floating platform).
- Mooring buffer zone: an area around each mooring line that should be kept clear. According to ISO 19901-7, the final anchor installation shall be at least 100 m from other offshore installations. Based on this, we set a 50 m buffer radius around the anchors and mooring lines, ensuring a 100 m safety distance between the mooring systems of different turbines.
- Lease area boundary: a polygonal lease around boundary, defined by x and y coordinates.

The buffer areas for the wind turbine and moorings are illustrated in Figure 3.

### *2.4. Optimization*

The overall optimization objective function is levelized cost of energy (LCOE); however, we break that down into AEP and mooring system capital cost to focus on what is affected by the layout.

Annual energy production (AEP) is computed from FLORIS based on the layout, using the thrust and power curves of the IEA 15-MW reference turbine. Floating platform displacements, pitch angles, and dynamic motions are not considered in the AEP calculation. Platform pitch and dynamic motions tend to have similar effects on all turbines and therefore have little influence on the layout optimization. Because the mooring systems are taut and have evenly spaced line headings, the platform offsets will be small and in a similar downwind direction for all turbines, meaning that platform offsets will have a minimal effect on wake losses and can be reasonably neglected. This may not be the case for other mooring systems (see [12]).

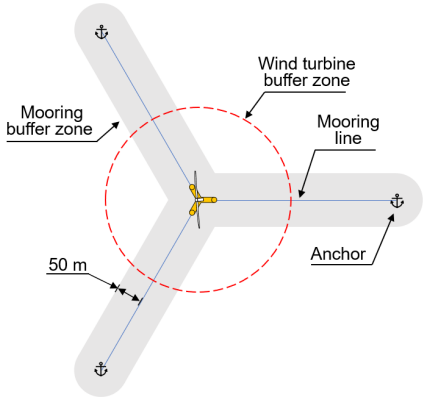


Figure 3: Spatial boundaries around a wind turbine

Mooring system cost is broken down into a cost per length of mooring line, whose length depends on the water depth, and a cost per anchor, which includes installation cost and depends on the soil type at the anchor position. In this way, there is spatial dependence to the objective function regardless of whether it is AEP, cost, or a proxy for LCOE.

We use the sequential least squares quadratic programming (SLSQP) method in Python's SciPy package to optimize the layout. The spatial constraints are implemented with constraint functions that compute the amount of surface area of a buffer zone (Figure 3) that is overlapping a boundary or another buffer zone. The mooring or turbine buffer areas are applied as constraints with each other (a mooring buffer area can't cross another mooring buffer area, and a turbine buffer area can't cross another turbine buffer area). Also, each of these buffers is not permitted to cross the lease around boundary. The rationale is that a minimum distance should be kept between turbines and a minimum margin between mooring lines, as well as the lease area boundary. A mooring buffer and turbine buffer can cross each other, since the former pertains to underwater components while the latter is above the water. The different constraint scenarios are illustrated in Figure 4.

## 3. Results

We test this optimization approach on a sample scenario involving 6 turbines in a 7-km by 8-km area. The turbines are the IEA 15 MW offshore reference wind turbine [20] on the VolturnUS-S semisubmersible platform [21]. We consider taut polyester mooring lines with a declination angle of 30 degrees. The seabed has a consistent slope in the x direction and some camber in the y direction so that there is a shallow area that will offer decreased mooring costs. To add spatial complexity, we include an area of bedrock, represented by an increased anchor cost, which can be seen in Figure 7. The presence of rock versus mud is defined at each 500-m grid node with bilinear interpolation between nodes as an initial approximation. In the results that follow, we use the assumptions detailed in Table 1 and the wind rose shown in Figure 1a.

Four sets of results follow: an AEP maximization on a uniform seabed, a mooring cost minimization over a nonunifrom seabed, the same minimization when there is an area of rock requiring more expensive anchors, and an LCOE minimization that includes both seabed variation and wake effects. We run each optimization for 30 iterations of the SLSQP algorithm, which entails just under 600 function evaluations. The first and last optimizations, which use FLORIS, take around 20 minutes. The others take around 30 seconds. An initial rectangular array layout with 2000-m spacings between turbines provides the starting point for the optimization. We then run the optimization, adjusting the position of each turbine and the heading of each mooring system, with sub-adjustments of the moorings based on their

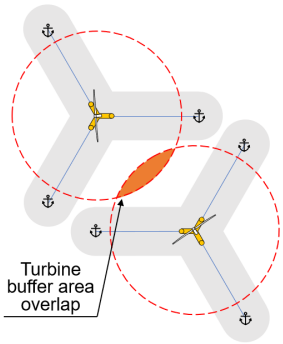


(a) Overlap between buffer areas of adjacent turbines

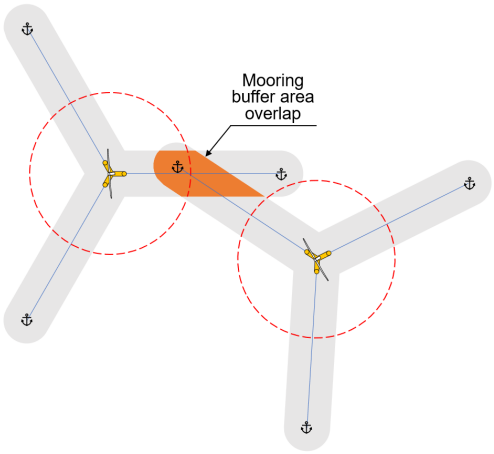


(b) Overlap between buffer areas of adjacent moorings

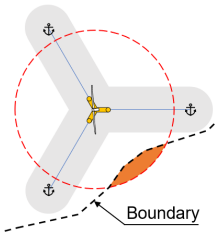


(c) Turbine buffer area crossing lease area boundary

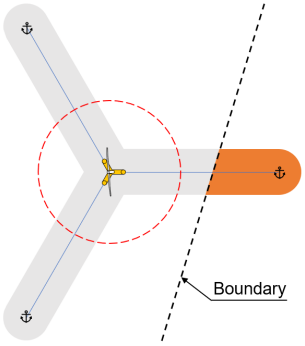


(d) Mooring buffer area crossing lease area boundary

Figure 4: Turbine and mooring spatial constraints

Table 1: Scenario assumptions

| Parameter | Value |
|---|---|
| Mooring line declination angle (deg) | 30 |
| Mooring line material | 142 mm polyester rope |
| Mooring line cost per unit length ($/m) | 165 |
| Anchor total cost for mud ($/anchor) | 300,000 |
| Anchor total cost for rock ($/anchor) | 500,000 |

changing positions over the seabed grid.

### *3.1. Maximizing AEP Considering Layout Constraints and Wakes*

This case considers the polygonal lease area and the spatial constraints detailed in Section 2. The objective is to maximize AEP, which is calculated at each design point using FLORIS. The initial regular layout and the optimized layout are shown in Figure 5.

The results show that the AEP is improved by 2.0% by spreading out the turbines as much as possible within the area, including mooring line orientations that allow the turbines to be closer to the boundaries. Most turbines are seen to be up against the boundary, indicating that the spatial constraints with the boundary are holding.

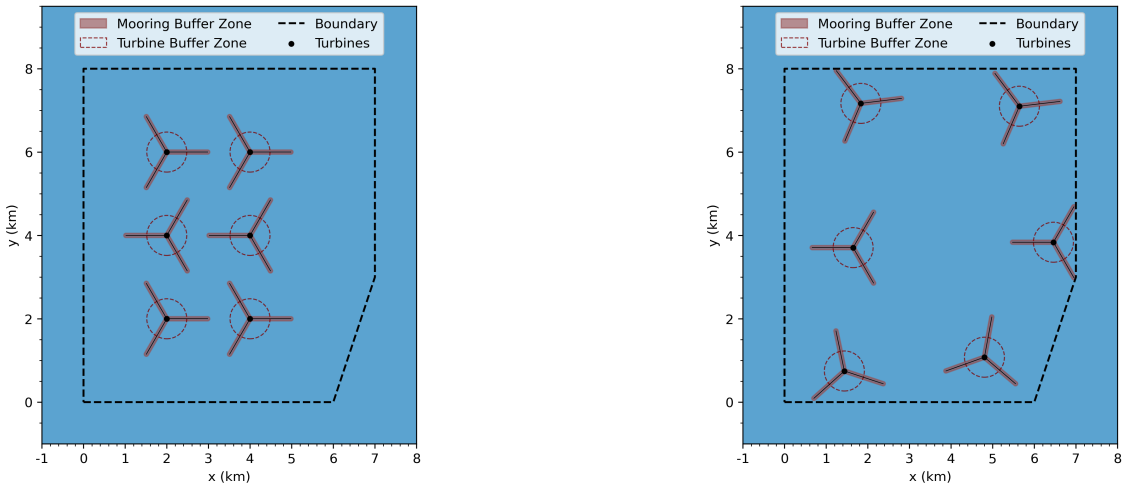


(a) Initial layout (b) Optimized layout

Figure 5: Minimizing wake losses on uniform seabed (2.0% AEP increase).

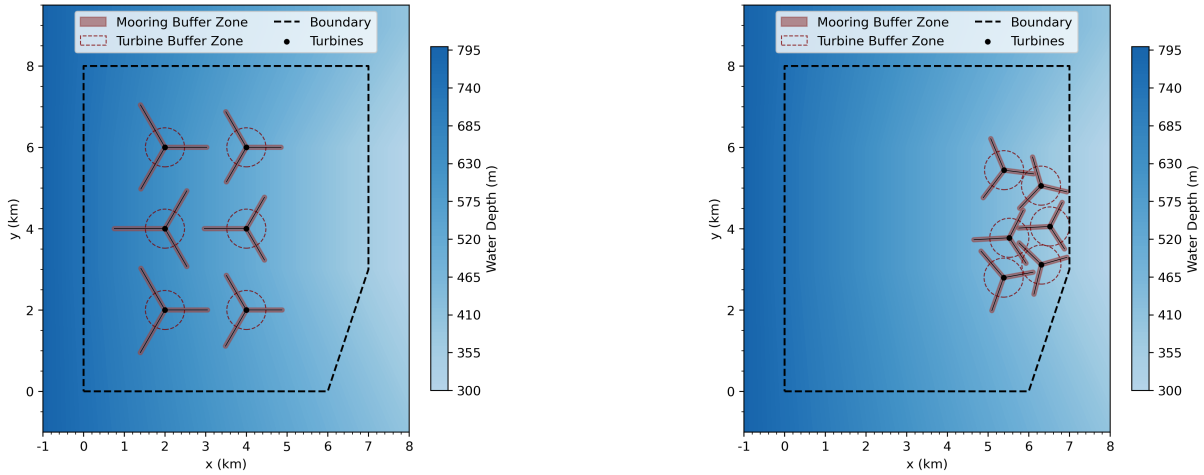


(a) Initial layout (b) Optimized layout

Figure 6: Minimizing CapEx on sloped seabed (11% mooring cost reduction).

*3.2. Minimizing Cost Considering Layout Constraints and Seabed Variability*

This case focuses on the effect of seabed variability on the mooring system size and cost. The goal is to minimize the total mooring system cost; wake effects are not considered. Because the anchoring radius changes with water depth, the spatial constraints also change with depth.

The first example, shown in Figure 6, deals with a sloped seabed, where depth is the only factor driving the objective function (mooring system cost). The results show a clear clustering of the turbines into the shallowest region of the area and achieve a cost reduction of 11%. As before, the boundary constraints are holding. In addition, the constraints between turbines are seen to be holding. There are some cases where mooring buffer zones are up against each other, and others with the turbine buffer zones. The results show how both constraints are effective and can come into play depending on the headings of the mooring lines.

The second example (Figure 7) adds a region on the seabed, such as rock, where more expensive anchor types would be required. We modeled this as a 67% increase in the cost of

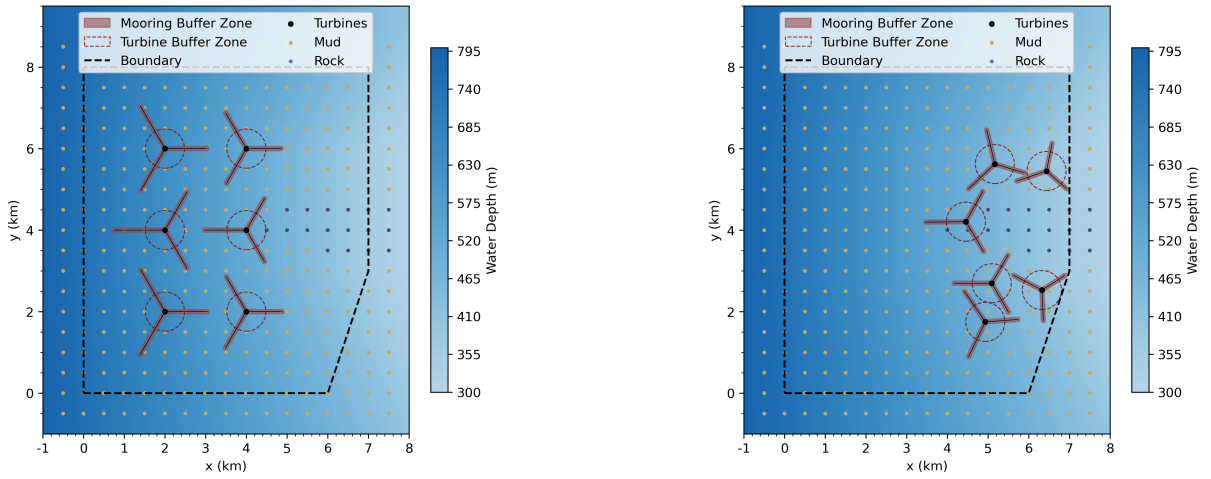


(a) Initial layout (b) Optimized layout

Figure 7: Minimizing CapEx on sloped seabed with varied soil (8.7% mooring cost reduction).

any anchors falling in that region. The results show that the turbine anchor positions avoid this area entirely. The turbines move to the shallowest locations outside of this area, achieving a cost reduction of 8.7%, slightly less than the previous case. As before, the spatial constraints are respected. There is also an indication that the turbine positions can become "stuck" by local spatial constraints and unable to move to other positions that may be globally better (see for example the lowest turbine in Figure 7b).

### *3.3. Minimizing LCOE Considering Layout Constraints, Seabed Variability, and Wakes*

This case combines the factors from previous cases. As a proxy for LCOE, the objective function is the mooring system cost divided by the AEP. The optimized layout (Figure 8) shows a combination of the behaviors seen previously.

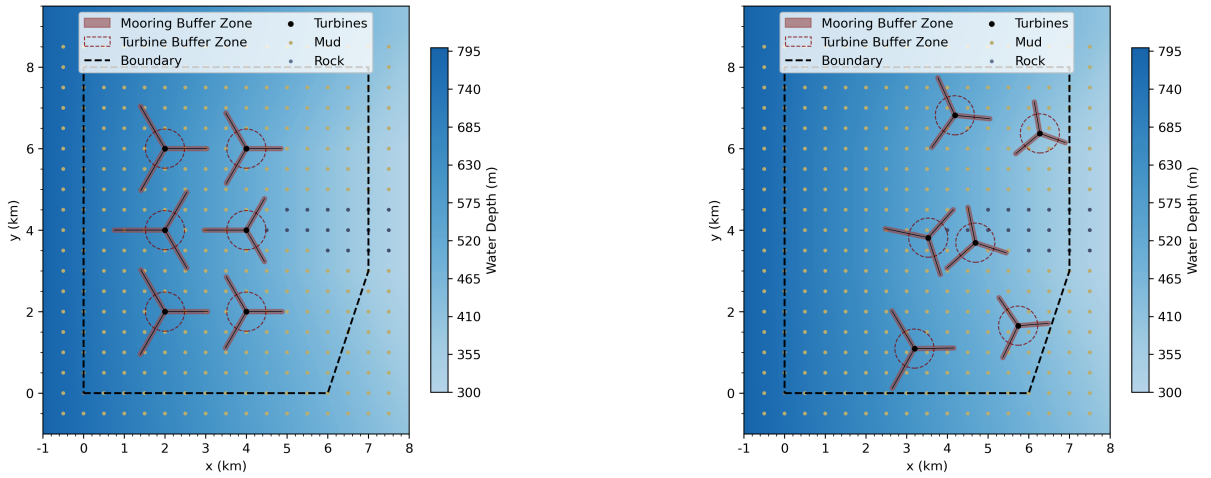


(a) Initial layout (b) Optimized layout

Figure 8: Minimizing LCOE on sloped seabed with varied soil (0.9% AEP increase, 5.5% mooring cost decrease, 6.4% LCOE decrease).

The turbines shift toward shallower water to reduce cost (by 5.5%), but they also stay spread out to mitigate wake losses (to improve AEP by 0.9%). The two turbines in the middle are close together but they avoid any anchor placement in the rocky area of the seabed.

### *3.4. Discussion*

Table 2 lists the results of each case in terms of AEP, total mooring system cost, maximum mooring line cost (based on the longest line), maximum anchor cost (based on the closest anchor to the rock region), and proxy LCOE. These results show the expected trends, where maximizing AEP gives the largest AEP, while minimizing cost gives the lowest AEP because of how tightly the turbines are packed in the shallow area. The mooring system costs also follow a predictable trend, where the initial layout has the highest cost, while optimizing to minimize cost successfully positions the moorings as shallow as possible and gives the lowest mooring cost. When minimizing the proxy for LCOE, which involves both cost and AEP, both the cost reduction and AEP increase fall in between those of the other cases, illustrating the tradeoffs between those objectives. Figure 9 compares the layouts.

Table 2: AEP, cost, and LCOE proxy results from six cases (f: flat, s: slope, r: rock)

| | AEP | | Mooring total | | Max. line | | Max. anchor | | LCOE proxy | |
|---|---|---|---|---|---|---|---|---|---|---|
| | (GWh) | (Δ%) | (k$) | (Δ%) | (k$) | (Δ%) | (k$) | (Δ%) | ($/MWh) | (Δ%) |
| Initial (f) | 375 | 0.0 | 8566 | -2.4 | 176 | -22.1 | 300 | 0.0 | 22.85 | -2.4 |
| Max. AEP (f) | 382 | 2.0 | 8566 | -2.4 | 176 | -22.1 | 300 | 0.0 | 22.41 | -4.3 |
| Initial (s) | 375 | 0.0 | 8778 | 0.0 | 226 | 0.0 | 300 | 0.0 | 23.41 | 0.0 |
| Min. cost (s) | 355 | -5.3 | 7801 | -11.1 | 155 | -31.4 | 300 | 0.0 | 21.96 | -6.2 |
| Min. cost (s+r) | 369 | -1.5 | 8012 | -8.7 | 176 | -21.9 | 315 | 4.9 | 21.70 | -7.3 |
| Min. LCOE (s+r) | 378 | 0.9 | 8295 | -5.5 | 201 | -10.8 | 302 | 0.7 | 21.92 | -6.4 |

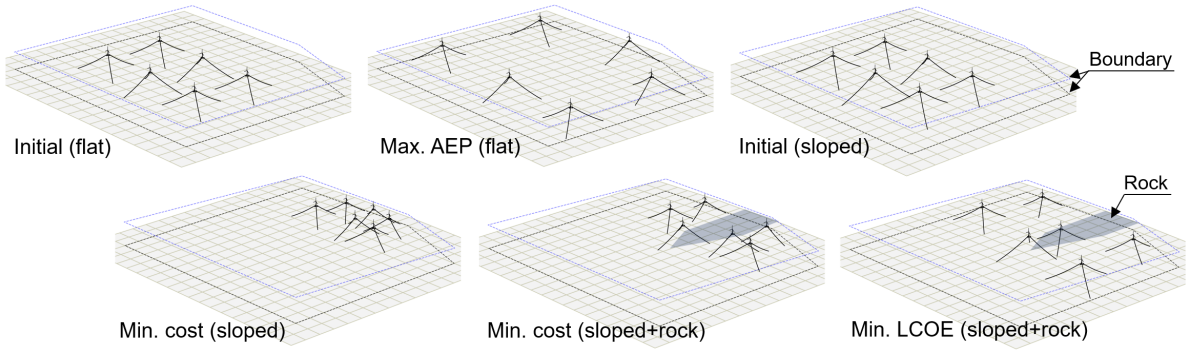


Figure 9: MoorPy three-dimensional model of the layouts in Table 2

## 4. Conclusions

This work presents a method for including site-specific mooring designs in the layout of optimization of a floating wind farm over a heterogeneous seabed. The results demonstrate that AEP gains and cost reductions can be achieved depending on the choice of objective function, with an LCOE-type optimization successfully balancing improvements in both AEP and cost. The impacts of wake losses, turbine and mooring buffer zones, and seabed variations are clear.

The presented results are informative in showing layout optimization behaviors and the success of the method. However, they also indicate potential weaknesses, such as when a local

constraint appears to block motion towards a global optimum. These challenges would likely compound with more turbines and more complex scenarios involving real seabed characteristics. Early optimizations in such cases did not converge to feasible solutions reliably. A related challenge is that real seabeds can have very abrupt changes in bathymetry or soil type, which can overly constrain the search space of a gradient based optimizer. Gradient-free optimization algorithms (such as Particle Swarm Optimization) could help overcome these challenges and enable more versatile and large-scale layout optimization, but much more investigation is needed.

Future work will explore improved optimization algorithms on larger-scale scenarios, and will also consider optimizing regular turbine layouts, where a rectangular grid is assumed and only its spacing and orientation are varied. These efforts can enable more comprehensive comparison studies of different layout alternatives for floating wind farms, as well as their suitability and sensitivity to realistic seabed conditions and lease area boundaries.

## Acknowledgments

This work was authored by the National Renewable Energy Laboratory, operated by the Alliance for Sustainable Energy, LLC, for the U.S. Department of Energy (DOE) under Contract No. DE-AC36-08GO28308. Funding provided by the DOE Office of Energy Efficiency and Renewable Energy Wind Energy Technologies Office. The views expressed in the article do not necessarily represent the views of the DOE or the U.S. Government. The U.S. Government retains and the publisher, by accepting the article for publication, acknowledges that the U.S. Government retains a nonexclusive, paid-up, irrevocable, worldwide license to publish or reproduce the published form of this work, or allow others to do so, for U.S. Government purposes.

## References

[1] Mosetti G, Poloni C and Diviacco B 1994 *Journal of Wind Engineering and Industrial Aerodynamics* **51** 105–116
[2] Chen Y, Li H, He B, Wang P and Jin K 2015 *Energy Conversion and Management* **105** 1318–1327
[3] Criado Risco J, Valotta Rodrigues R, Friis-Møller M, Quick J, Mølgaard Pedersen M and Réthoré P 2023 *Wind Energy Science Discussions* 1–24
[4] Stanley A P J, Roberts O, King J and Bay C J 2021 *Wind Energy Science* **6** 1143–1167
[5] Thomas J J, Baker N F, Malisani P, Quaeghebeur E, Sanchez Perez-Moreno S, Jasa J, Bay C, Tilli F, Bieniek D, Robinson N, Stanley A P J, Holt W and Ning A 2023 *Wind Energy Science* **8** 865–891
[6] Díaz H, Silva D, Bernardo C and Guedes Soares C 2023 *Renewable Energy* **204** 449–474
[7] Liu Z, Fan S, Wang Y and Peng J 2021 *Energy Conversion and Management* **245** 114610
[8] Perez-Moreno S S, Dykes K, Merz K O and Zaaijer M B 2018 *Journal of Physics: Conference Series* **1037** 042004
[9] Cazzaro D, Koza D F and Pisinger D 2023 *European Journal of Operational Research* **311** 301–315
[10] Rapha J I 2023 Floating offshore wind farm layout optimisation DOI: 10.5281/zenodo.8328029
[11] Lerch M, De-Prada-Gil M and Molins C 2021 *Int'l Journal of Electrical Power & Energy Systems* **131** 107128
[12] Mahfouz M Y and Cheng P 2023 *Wind Energy* **26** 251–265
[13] Froese G, Ku S Y, Kheirabadi A C and Nagamune R 2022 *Renewable Energy* **190** 94–102
[14] Liang Z and Liu H 2023 *Ocean Engineering* **283** 115098
[15] Serrano González J, Burgos Payán M, Riquelme Santos J M and González Rodríguez G 2021 *Energies* **14** 886 number: 4
[16] Hietanen A I, Snedker T H, Dykes K and Bayati I 2023 *Wind Energy Science Discussions* 1–31
[17] Hall M, Housner S, Sirnivas S and Wilson S 2021 MoorPy (Quasi-Static mooring analysis in python) DOI: 10.11578/DC.20210726.1 URL `https://www.osti.gov/doecode/biblio/61138`
[18] Gebraad P, Fleming P, Ning A and van Wingerden J 2014 FLORIS URL `https://www.osti.gov/biblio/1262644`
[19] King J, Fleming P, King R, Martínez-Tossas L A, Bay C J, Mudafort R and Simley E 2021 *Wind Energy Science* **6** 701–714
[20] Gaertner E *et al.* 2020 Definition of the IEA 15-Megawatt offshore reference wind turbine Tech. Rep. NREL/TP-5000-75698
[21] Allen C *et al.* 2020 Definition of the UMaine VolturnUS-S reference platform developed for the IEA wind 15-Megawatt offshore reference wind turbine Tech. Rep. NREL/TP-5000-76773